Low Overhead Control Channels in Wireless Networks

Eugene Chai and Kang G. Shin
Real-Time Computing Laboratory
Department of Electrical Engineering and Computer Science
The University of Michigan, Ann Arbor, MI 48109-2121, U.S.A.
{zontar, kgshin}@eecs.umich.edu

Abstract

Low-latency, low-overhead and reliable control channels are essential to the efficient operation of wireless networks. However, control channels that utilize current in-band and out-of-band designs do not fully meet this requirement. In this paper, we design and implement Aileron, a novel control channel based on automatic modulation recognition that carries control frames over an OFDM(A) PHY by varying the modulation rate of the OFDM subcarriers. Under Aileron, the control information is embedded into the *modulation type*, not as the actual symbol value. Aileron has three important advantages: (a) control frame exchange without frame synchronization, (b) signaling with low bandwidth overhead, and (c) resilience to channel errors.

We have evaluated Aileron using both extensive simulations and real-world measurements, and discovered that control frames can be transmitted with more than 80% accuracy using only 10 OFDM blocks on a channel with SNR of merely 10dB.

1 Introduction

Dynamic spectrum management is a well-known approach to increasing the throughput and utilization of high-bandwidth WLANs [1, 2]. However, this approach to spectrum usage amplifies two aspects of wireless networks:

Multi-channel transmissions. Wireless devices must combine multiple fragmented spectrum bands [1, 3] to get sufficient bandwidth to meet high throughput demands. Devices must reconfigure their channel usage on a per-session [1] or even on a per-frame [2] basis. This is an abrupt departure from the current 802.11 infrastructure WLANs where AP channels are fixed during deployment and rarely changed.

Partially overlapping channels. Dynamic spectrum use increases the probability of interference between transmissions on partially overlapping channels. These interfering frames cannot be decoded correctly, thus preventing any channel access mechanisms, beyond those based on basic energy sensing, from being employed.

Unfortunately, control channels in these networks (e.g. RTS/CTS, beacon frames, network management frames
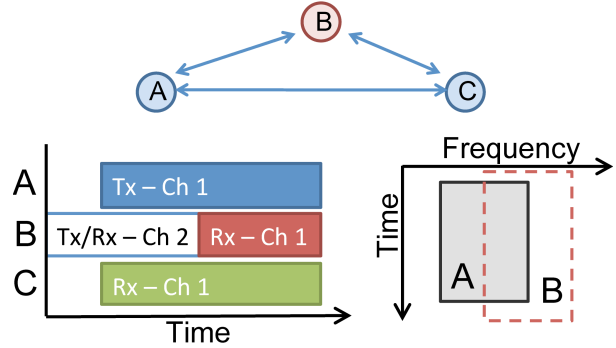

Figure 1: (Top) Network of 3 nodes; *B* is Aileron-enabled (Bot Left) Multi-channel WLAN: *B* recovers the modulation types from the partially overheard frame from *A* to *C*. (Bot Right) Partially overlapping channels: *A* and *B* are on partially overlapping channels. *B* recovers the modulation types from only a fraction of the subcarriers used by *A*.

etc.) have a severe limitation: all the nodes that are exchanging control messages must be on the same channel. As a result, exchange of control messages must be synchronized in time, as done in FICA [2], or coordinated over a known and fixed set of control channels, as is the case of Jello [1] and CMAC [4].

In this paper, we present Aileron, a novel control channel design for multi-channel OFDM networks. Aileron encodes information using *modulation types* of individual subcarriers: binary, quadrature and eight phase shift keying (BPSK, QPSK and 8PSK) along with 16 and 64 quadrature amplitude modulation (16QAM and 64QAM). This is in stark contrast to typical digital communication techniques that encode information into *symbol values*.

To understand how Aileron works, consider the case where BPSK, QPSK, and 8PSK are mapped to values 0, 1, and 2, respectively. A transmitter that needs to send an integer-valued control message first converts the base-10 integer to a ternary number; the modulation rate of each subcarrier is then set according to the value of its corresponding ternary digit. At the receiver, the control frame can be recovered by recognizing the modulation rate of each subcarrier and reconstructing the corresponding ternary number.

Aileron has several important features that meet the demands of wireless networks:

Asynchronous out-of-band signaling. Aileron can simultaneously transmit both control and data messages to *different* receiving nodes; this is known as the *active mode* of Aileron. The data frame is transmitted using standard PHY/MAC protocols between two directly connected nodes; the control message is transmitted using modulation encoding to an *out-of-band* node.

Figure 1 illustrates two examples of asynchronous Aileron in action: Aileron in multi-channel WLANs and Aileron in partially overlapping channels. In multi-channel WLANs, consider an example with three nodes *A*, *B* and *C* on channels 1, 2 and 1 respectively. *A* and *B* are in-band directly connected nodes while *C* is the out-of-band node. If *B* switches back to channel 1 in the middle of a frame transmission from *A* to *C*, it cannot decode the frame and any control message broadcasted by *A* is missed by *B*; this control message will have to be retransmitted, thus wasting bandwidth. With Aileron, *A* can tag the entire frame with a single ternary-valued control message; *B* can then recover this control message using any subset of symbols from the data frame.

Asynchrony also enables Aileron to exchange frames between nodes on partially overlapping channels; this is in stark contrast to typical PHY/MAC protocols that require communicating nodes to share the same channel. Consider two nodes *A* and *B* (Figure 1) that are on partially overlapping channels. With Aileron, *A* embeds control information in the modulation rates of subcarriers shared between the two channels; *B* can subsequently recover the message from these overlapping subcarriers.

Note that Aileron is not as useful for signaling between directly connected nodes, such as *A* and *C* in Figure 1 under the multi-channel scenario, since *A* and *C* can directly exchange control frames using the standard PHY/MAC protocol.

Multi-protocol support. Active mode Aileron can be supported by multiple protocols with minimal modifications. *Passive mode* Aileron, on the other hand, enables the integration of an Aileron-enabled node into wireless networks without any modifications to other existing devices. In passive mode, Aileron functions as a modulation identifier for each subcarrier of an OFDM frame. Consider the two scenarios in Figure 1 again, except that now *A* and *C* are unmodified WLAN devices while *B* is an Aileron node. In both the multi-channel and partially overlapping channel situations, *B* identifies the modulation rate of the individual subcarriers. Furthermore, *B* can infer the channel state between *A* and *C* because the modulation rate is typically selected by an auto-rate algorithm to match the estimated channel conditions [5]. This allows Aileron to be used in any OFDM-based wireless network (e.g. WiMAX, LTE) without the need for a compatible PHY implementation.
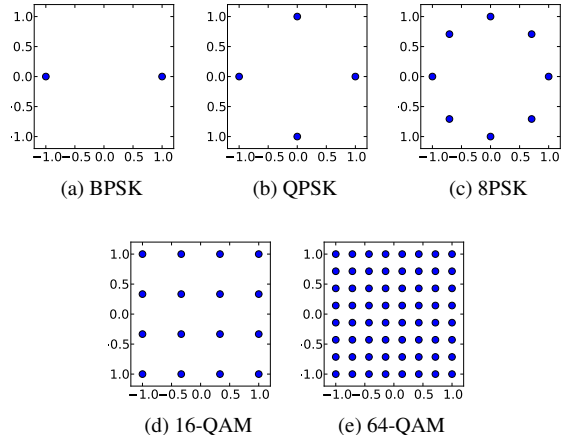

(a) BPSK   (b) QPSK   (c) 8PSK

(d) 16-QAM   (e) 64-QAM

Figure 2: Phase-Shift Keying (PSK) and Quadrature Amplitude Modulation (QAM) constellations that are recognized by Aileron.

Resilience to errors. Our evaluations, using both simulations and actual measurements, show that the signaling information can be decoded at SNR levels as low as 10dB with 99% accuracy. Furthermore, mobility does not have any significant impact on the decoding accuracy. This makes Aileron useful for highly mobile (e.g., cellular) networks that operate in challenging environments with severe fading and multipath effects.

Our contributions can be summarized as follows. First, we design a reliable, low-overhead PHY modulation-based signaling scheme, Aileron, that does not require frame synchronization. Second, we implement Aileron on a USRP2 platform and demonstrate via experimentation its efficiency and reliability. We also evaluate the scheme under a wide range of channel conditions, demonstrating its superior performance under varying channel and mobility conditions. Third, Aileron is applied to improve air-time fairness in FICA without any additional channel contention overhead.

The paper is organized as follows. Sec. 2 gives an overview of Aileron. §3 describes the key ideas and techniques behind synchronization-free signaling, while §3 details the modulation-based signaling. §4 evaluates Aileron under simulated conditions. §6 discusses related work while §7 concludes the paper.

2 Aileron Overview

Constellation diagrams. Figure 2 shows the five constellation diagrams of the constellations recognized by Aileron: BPSK, QPSK, 8PSK, 16QAM and 64QAM. In each constellation diagram, each point is used to encode $\log_2(M)$ bits, where M is the total number points
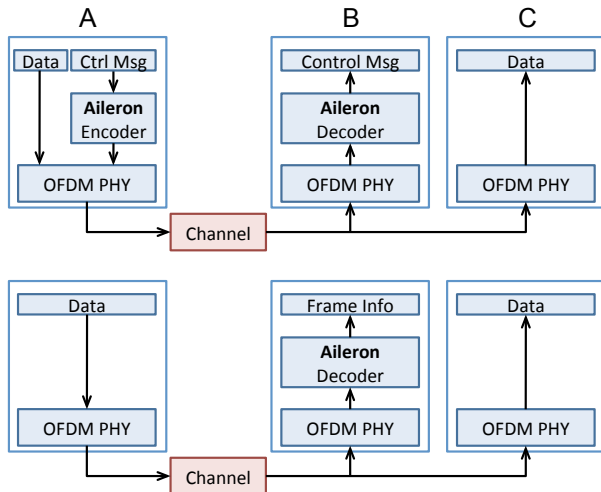
Figure 3: Architectural block diagrams of Aileron. (Top) Active-mode. *A* is an Aileron-enabled (WLAN) transmitter while *C* is an unmodified (WLAN) receiver; *B* is a Aileron-enabled receiver. (Bottom) Passive-mode. *A* and *C* are unmodified (WLAN) devices while *B* is an Aileron node.

in the diagram. For an arbitrary subcarrier, the constellation diagram chosen to encode its bits determines its modulation rate. The PSK and QAM constellations in Figure 2 are each chosen such that lower-level modulations are subsets of higher-level modulations—the QPSK constellation includes the two points of the BPSK constellation, and similarly, the 8PSK constellation contains the points in both QPSK and BPSK. QAM constellations differ from the PSK constellations in that no constellation point exists along the in-phase and quadrature-phase axes. However, QAM constellations still maintain the subset property, with 16-QAM being a subset of 64-QAM, although no QAM constellations are subsets of any PSK constellation, and vice versa.

Active-mode Aileron. Figure 3 illustrates the architecture of the Aileron transmitter and receiver of the example 3-node network in Figure 1. The transmitter, node *A*, contains an Aileron encoder module that maps the control message into the modulation rates of the *Aileron subcarriers*. The modulation rates of these subcarriers are limited to BPSK, QPSK and 8PSK, which correspond to the a ternary basis 0, 1 and 2; subcarriers that are not used for Aileron signaling (i.e. non-Aileron-subcarriers) are not restricted to the these constellations. Additionally, the subcarrier that precedes the Aileron subcarrier must be forced to the BPSK modulation. This is done to accomodate the OFDM symbol acquisition algorithm of Aileron that will be explained in §3. The OFDM PHY at *A* uses these selected modulation rates to generate the OFDM frame that it transmits to *C*. The Aileron decoder at *B* recovers the control message from the symbols received by the OFDM PHY from a multi-channel or par-

tially overlapping transmission.

For example, consider a set of 6 consecutive OFDM subcarriers, within the same 802.11g OFDM symbol, $p_1, \ldots, p_6$ used to represent a ternary value with p_1 being the least significant ternary digit. Assume that BPSK, QPSK and 8PSK map to integers 0, 1 and 2, respectively. In order to encode the base-10 number 7_{10} to 012_3, we set the non-Aileron-subcarriers p_1, p_3 and p_5 to be BPSK-modulated, and set the Aileron-subcarriers p_2, p_4 and p_6 to be BPSK, QPSK, and 8PSK-modulated, respectively.

Passive-mode Aileron. In passive-mode Aileron, *A* and *C* are unmodified wireless devices while *B* is a Aileron device. Hence, all data subcarriers in the OFDM frame will have the same modulation rate. The Aileron decoder in *B* identifies the subcarrier modulation rates from the OFDM symbols recovered by the PHY. Aileron can differentiate BPSK, QPSK, 8PSK; it can also differentiate between PSK and QAM, but cannot reliably identify 16QAM and 64QAM yet. The identification of 16QAM and 64QAM is the subject of on-going work.

Automatic Modulation Recognition In both passive and active Aileron, the Aileron decoder employs Automatic Modulation Recognition (AMR) [6] to determine the modulation of each subcarrier in a group of N identically modulated OFDM symbols. Let $S_k = \{s_{k,1}, \ldots, s_{k,N}\}$ be a sequence of received samples of the kth subcarrier of N consecutive OFDM symbols. These samples are modulated using a constellation $C = \{c_1, \ldots, c_M\}$ with M points. The group of N OFDM symbols must satisfy

$$\rho(s_{k,i}) = \rho(s_{k,j}), \ i \neq j, \ 1 \leq i,j \leq N, \ 1 \leq k \leq K. \quad (1)$$

where $\rho(s_{k,n})$ is the modulation rate of $s_{k,n}$ and K is the total number of subcarriers in each OFDM symbols. Note that it is possible for $\rho(s_{k,n}) \neq \rho(s_{k',n})$ when $k \neq k'$.

Data: S_k is a sequence of N constellation points
Result: Identified modulation
begin
  if `is_bpsk`(S_k) **then**
    | **return** "BPSK";
  else if `is_qpsk`(S_k) **then**
    | **return** "QPSK";
  else if *Active-mode or* `is_8psk`(S_k) **then**
    | **return** "8PSK";
  else
    | **return** "QAM";
  end
end

Algorithm 1: Automatic modulation recognition.

The method used for differentiating between these modulations is shown in Algorithm 1. Each of the mod-
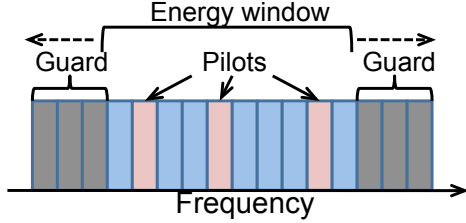
Figure 4: OFDM symbol that consists of three different types of subcarriers: data, pilot and guard subcarriers. An energy window is slid over the subcarriers to find the coarse frequency offset.

ulation rates—BPSK, QPSK and 8PSK—has an associated decision rule, indicated by the functions is_bpsk, is_qpsk and is_8psk, respectively. Active-mode Aileron only uses BPSK, QPSK and 8PSK: it matches the signal samples against the BPSK and QPSK rules; if the samples match neither of these rules, the modulation is declared to be 8PSK. Passive-mode Aileron matches the signal against all three rules and if no match is found, the modulation of samples is declared to be "QAM". Passive-mode Aileron does not differentiate between 16QAM and 64QAM because the constellation points of QAM are encoded using both magnitude and phase; it is not possible to accurately recover the magnitude without proper calibration using the frame preamble. On the other hand, because it is easy to differentiate between the three PSK schemes, we will restrict the allowable modulation schemes in active-mode Aileron to the PSK modulations to improve signaling reliability.

3 Aileron Algorithm Details

3.1 How does Aileron acquire an OFDM symbol?

Aileron identifies subcarrier modulation rates from the OFDM symbols that are recovered from arbitrary locations of the transmitted frame. These symbols must be received without any help from the typical preamble-based frame detection and synchronization routines that accompany standard PHY receiver protocols. In this section, we describe the process of recovering these frames with sufficient accuracy for the modulation of each subcarrier to be identified.

An OFDM block in the time domain is acquired in two steps: frequency correction and timing acquisition. The frequency drift θ encountered in an OFDM block can be expressed as $\theta = \Omega + \varepsilon$, where Ω is the *coarse* frequency drift component and is an integer multiple of the subcarrier bandwidth; ε is the *fine* frequency drift component and is smaller than the bandwidth of a subcarrier. We employ a maximum-likelihood acquisition algorithm [7] to both acquire the symbol and correct its fine-frequency

drift. The OFDM symbol is identified from the autocorrelation peak between the symbol and its cyclic prefix; this cyclic prefix is a copy of the last few samples of an OFDM symbol that have been pre-pended to the symbol. In order to correct the coarse frequency drift, we slide a window with a bandwidth equal to that of the data and pilot subcarriers over all subcarriers of the OFDM symbol, as shown in Figure 4. At each window position, the energy of all subcarriers within the window is summed. The offset of the window, from its ideal central position, with the highest total energy from the subcarriers is the coarse frequency offset Ω.

The OFDM acquisition algorithm in [7] cannot guarantee that perfect timing recovery is always achieved. This timing recovery error induces a phase error in the subcarriers, due to the known property of DFTs: a timing offset of l samples introduces a phase error of $e^{-j2\pi kl/M}$ in the kth subcarrier. The corrected symbol Y_k in the kth subcarrier is obtained using the relation:

$$Y_k = X_k \cdot X_{k-1}^* / |X_{k-1}| \tag{2}$$

where the $(\cdot)^*$ operator denotes the complex conjugate and X_k is the uncorrected symbol in the kth subcarrier. If the symbols X_k and X_{k-1} are from the same constellation, then this correction will preserve the modulation scheme for subsequent recognition by Aileron. For example, if X_k and X_{k-1} are modulated using QPSK, then Y_k will definitely be one of the QPSK constellation points. However, the actual constellation point held by X_k is lost, thus preventing the original bit content from being recovered. This does not have any effect on the performance of Aileron since only the modulation type is of interest.

3.2 What are the decision rules?

Consider a sequence of subcarrier values S_k modulated using a modulation C. The normalized mean squared error between the received samples and the ideal constellation points is

$$\text{MSE}_C(S_k) = \frac{1}{N} \sum_{n=1}^{N} \left(\min_{c_m \in C} \left\{ \frac{s_{k,n}}{|s_{k,n}|} - \frac{c_m}{|c_m|} \right\} \right)^2. \tag{3}$$

The normalization of S_k and C minimizes errors due to the randomly varying magnitude of the received samples.

A straightforward approach to recognizing PSK modulations is to use the fact that each received, distorted PSK modulation will have the smallest MSE when compared with its ideal constellation. For example, if a received sequence S_k is BPSK modulated, then $\text{MSE}_{\text{BPSK}}(S_k)$ will be smaller than all other $\text{MSE}_C(S_k)$ with $C \neq \text{BPSK}$. This is the principle employed in [8] for differentiating between PSK modulations. However, this approach does not allow us to differentiate PSK from
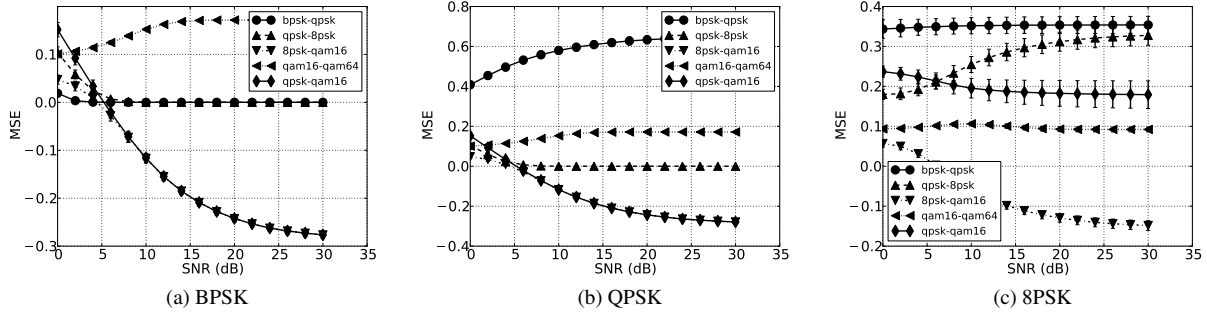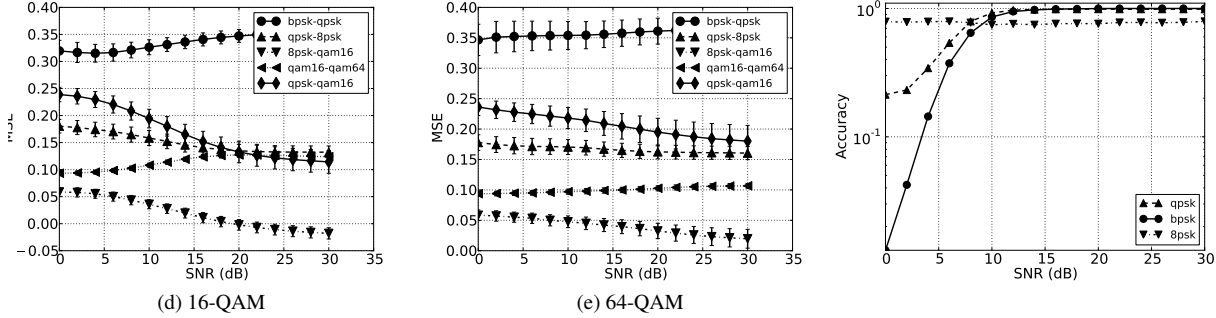
(a) BPSK (b) QPSK (c) 8PSK

Figure 5: Differences in MSE values for input sequences of different modulation rates

(d) 16-QAM (e) 64-QAM

Figure 6: Accuracy of active-mode Aileron over a simulated channel with no doppler shift and an AMR window of 10.

Figure 5: Differences in MSE values for input sequences of different modulation rates

QAM modulations accurately. QAM constellations contain significantly more points than PSK constellations, thus making it easier for a received sequence of PSK-modulated symbols to have a smaller MSE with respect to QAM than to other PSK schemes.

The decision rule of each modulation scheme is based on the *difference* between the MSE of S to various constellations C:

$$\Gamma_{C_1,C_2}(S) \triangleq \mathrm{MSE}_{C_1}(S) - \mathrm{MSE}_{C_2}(S). \qquad (4)$$

Figure 5 shows the mean and standard deviation of the difference in MSE of the received symbols of each supported modulation scheme with respect to the ideal constellations. For every supported modulation, we transmit 320 symbols using 10 OFDM blocks of 32 subcarriers each over an AWGN channel with varying SNR levels. This is repeated 10000 times for each SNR level and the corresponding mean and standard deviation are plotted. In each figure, we use the notation "$C_1 - C_2$" to represent $\Gamma_{C_1,C_2}(S)$.

In the rest of this section, we will use these figures to illustrate the rationale behind the decision rules for each of BPSK, QPSK and 8PSK modulation rates.

(a) Recognizing BPSK: The decision rule used to recognize received symbols that are modulated using BPSK

is

$$\Gamma_{16\mathrm{QAM},64\mathrm{QAM}}(S) \geq \Gamma_{\mathrm{BPSK},\mathrm{QPSK}}(S), \quad \text{and} \qquad (5)$$

$$\Gamma_{16\mathrm{QAM},64\mathrm{QAM}}(S) \geq \Gamma_{\mathrm{QPSK},8\mathrm{PSK}}(S), \quad \text{and} \qquad (6)$$

$$\Gamma_{16\mathrm{QAM},64\mathrm{QAM}}(S) \geq \Gamma_{8\mathrm{PSK},16\mathrm{QAM}}(S) \qquad (7)$$

By comparing Figure 5a to the other sub-figures in Figure 5, it is obvious that one of the defining characteristics of the BPSK modulation is the fact that the mean value of $\mathrm{MSE}_{16\mathrm{QAM}}(S) - \mathrm{MSE}_{64\mathrm{QAM}}(S)$ is greater than all other MSE differences at SNRs greater than 2dB. This is precisely the characteristic that is used in Eqs. (5), (6) and (7) to identify the BPSK modulation.

(b) Recognizing QPSK: The decision rule to recognize an input stream modulated using QPSK is

$$\Gamma_{\mathrm{BPSK},\mathrm{QPSK}}(S) \geq \Gamma_{16\mathrm{QAM},64\mathrm{QAM}}(S)$$
$$\geq \Gamma_{\mathrm{QPSK},8\mathrm{PSK}}(S), \quad \text{and} \qquad (8)$$
$$\Gamma_{16\mathrm{QAM},64\mathrm{QAM}}(S) \geq \Gamma_{8\mathrm{PSK},16\mathrm{QAM}}(S). \qquad (9)$$

The input symbols are first matched against the BPSK decision rule and the QPSK decision rule is only considered if the BPSK decision rule does not evaluate to true on the sequence of input symbols. Figure 5b shows the differences in MSE values of a QPSK input sequence with respect to the various ideal constellations. Obviously, the ideal BPSK constellation only contains half

5

the points of the QPSK constellation. Hence, the mean distance between the QPSK input symbols to BPSK constellation points is significantly larger than the distance to the QPSK constellation points, thus making the QPSK constellation a "better match" for the input symbols than the BPSK constellation. As a result, we now have the properties

$$\Gamma_{\text{BPSK,QPSK}}(S) \geq \Gamma_{\text{QPSK,8PSK}}(S), \text{ and} \quad (10)$$

$$\Gamma_{\text{BPSK,QPSK}}(S) \geq \Gamma_{\text{16QAM,64QAM}}(S). \quad (11)$$

that hold true for expected MSE values. Since the mean distance of the QPSK- and BPSK-modulated received symbols to the other constellations is largely similar, Eqs. (6) and (7) still hold. Hence, we obtain the QPSK decision rule by combining Eqs. (10), (11), (6) and (7).

(c) Recognizing 8PSK: The decision rule to recognize a sequence of input symbols modulated using 8PSK is

$$\Gamma_{\text{QPSK,8PSK}}(S) \geq \Gamma_{\text{QPSK,16QAM}}(S), \text{ and} \quad (12)$$

$$\Gamma_{\text{QPSK,16QAM}}(S) \geq \Gamma_{\text{16QAM,64QAM}}(S), \text{ and} \quad (13)$$

$$\Gamma_{\text{QPSK,16QAM}}(S) < 0, \text{ and} \quad (14)$$

$$|\Gamma_{\text{8PSK,16QAM}}(S)| \geq \alpha, \text{ and} \quad (15)$$

$$|\Gamma_{\text{QPSK,8PSK}}(S) - \Gamma_{\text{16QAM,64QAM}}(S)| \geq \beta. \quad (16)$$

The 8PSK decision rule is used after both the BPSK and QPSK decision rules have been evaluated to be false on the input symbols. Hence, the 8PSK decision rule only needs to differentiate 8PSK from 16QAM and 64QAM constellations. It is obvious from Figures 5c, 5d and 5e that at SNRs greater than 6dB, (12), Eqs. (13) and (14) represent the key characteristics of the mean MSE differences that distinguish 8PSK from 16QAM and 64QAM. However, also observe that with a 16QAM-modulated input sequence (Figure 5d), at SNRs greater than 18dB, the mean values of $\text{MSE}_{\text{QPSK}}(S) - \text{MSE}_{\text{8PSK}}(S)$, $\text{MSE}_{\text{QPSK}}(S) - \text{MSE}_{\text{16QAM}}(S)$ and $\text{MSE}_{\text{16QAM}}(S) - \text{MSE}_{\text{64QAM}}(S)$ are close enough such that Eqs. (12), (13) and (14) will hold true for a significant proportion of the actual MSE difference values, thus increasing the probability that 16QAM will be mis-recognized as 8PSK. To prevent this, Eqs. (15) and (16) ensure that these MSE differences must not be "too close" in order for the 8PSK modulation to be correctly identified, with the degree of closeness to be defined by the parameters α and β. In our evaluations, we have found that $\alpha = \beta = 0.03$ gives the highest accuracy in differentiating 8PSK from QAM constellations.

3.3 What is the appropriate size of N?

The variance of the MSE and the corresponding accuracy of Aileron depends on the length (N) of the input

sequence S_k — AMR accuracy improves with longer input sequences but at the cost of a longer recognition delay.

The *AMR window* refers to the number of OFDM symbols used by each iteration of the AMR algorithm; this directly affects the length (N) of the sequence of input symbols S to the MSE equation (3). With active-mode Aileron, since every signaling subcarrier can use a different modulation scheme, an AMR window of length N (i.e., N OFDM blocks) will only produce N input symbols from a single subcarrier position. On the other hand, with passive-mode Aileron, all the data subcarriers use the same modulation scheme, so an AMR window of length N will contain $N \cdot K$ input symbols, where K is the number of data subcarriers per OFDM symbol. In our evaluation of Aileron, we will study the effects of the AMR window length on its accuracy.

4 Evaluation Using Simulated Channels

In this section, we evaluate the accuracy of Aileron under a wide range of simulated channel conditions.

4.1 Experimental Setup

We implemented Aileron using an OFDMA PHY in GNURadio with the parameters as listed in Table 1. A single transmitter-receiver pair is used in this evaluation. The transmitted samples are filtered using a simulated channel in MATLAB, using the parameters in Table 2, before being passed to the receiver.

Aileron is evaluated using the following JTC [9] channel models in MATLAB: `jtcInResC`, `jtcInOffC`, `jtcInComC`, and `jtcOutUrbHRLAC` that correspond to Indoor residential C, Indoor office C, Indoor commercial C, and Outdoor urban high-rise areas—Low antenna C, respectively. Note that the variation of the doppler frequency from 0 to 800Hz in 80Hz increments correspond to movement speeds of 0 to 100m/s in increments of 10m/s at a center frequency 2.4GHz. The set of chosen channel models, doppler frequencies and SNRs represent a wide range of possible channel conditions under which the AMR algorithm has to operate. The SNR of the channel is representative of the interference seen on the channel. Due to space limitation, we will only present the evaluation results obtained using the `jtcInOffC` channel. The performance of Aileron under the other channel models are very similar.

4.2 Aileron Accuracy in Static Environments

Active-mode Aileron accuracy under different SNRs. Figure 6 shows the accuracy of active-mode Aileron over
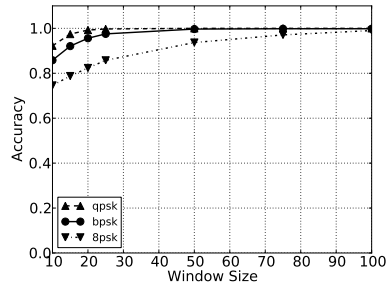
Figure 7: Accuracy of active-mode Aileron with different AMR window sizes, no doppler shift and a SNR of 10dB
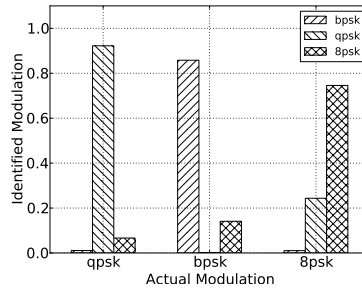
Figure 8: Active-mode Aileron recognition accuracy of modulation schemes with an AMR window of 10, a SNR of 10dB and no doppler shift.
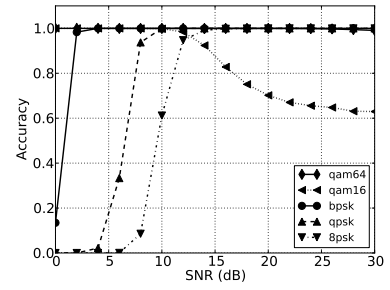
Figure 9: Passive-mode Aileron accuracy in a simulated channel with no doppler shift and an AMR window of size 10.
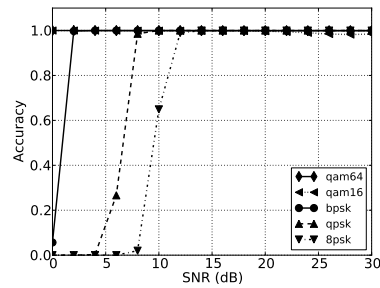
Figure 10: Passive-mode Aileron accuracy in a simulated channel with no doppler shift and an AMR window of 20.
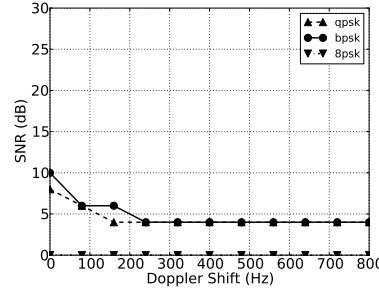
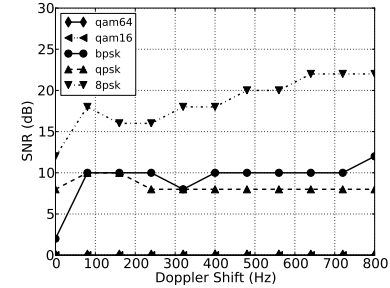Figure 11: Lowest SNR level at which the accuracy of active-mode Aileron exceeds 90%, using an AMR window of 50.

Figure 12: Lowest SNR level at which accuracy of active-mode Aileron exceeds 90%, using an AMR window of 10.

PHY Parameter	Value
Center frequency	2.4GHz
Total bandwidth	12.5MHz
Total subcarriers	1024
Cyclic prefix length	256
No. of subchannels	16
No. of subcarriers per subchannel	64
No. of active-mode signaling subcarriers per subchannel	6
No. of guard subcarriers per subchannel	32

Table 1: Parameters used in the OFDMA PHY.

Emulation Parameter	Value
Channel Model	jtcInResC, jtcInOffC, jtcInComC and jtcOutUrbHRLAC
Doppler Frequency	0 - 800Hz in 80Hz increments
Signal-to-Noise Ratio	0 - 30dB in 2dB increments
Modulation Rates	BPSK, QPSK, 8PSK, 16QAM and 64QAM
AMR Window	10, 15, 20, 25, 50, 75 and 100

Table 2: Parameters used in the emulated channels. The names of the channel model correspond to those used by MATLAB.

channels without mobility: symbols are sent over the fading channel with no doppler shift, which is representative of a typical indoor WLAN environment with almost no user and environmental mobility. This accuracy of Aileron is computed over 50000 AMR windows of 10 OFDM symbols each.

Aileron is shown to be able to recognize BPSK and QPSK modulations with practically perfect accuracy at SNR above 16dB. 8PSK is detected correctly approximately 79% of the time at all SNR levels. It must be emphasized that this level of accuracy is achieved using only *10 received symbols*. As expected, the active-mode Aileron detection accuracy increases as we increase the number of symbols used by the AMR.

Active-mode Aileron accuracy under different AMR window sizes. Figure 7 shows the AMR accuracy of active-mode Aileron when channel SNR and doppler shift are fixed at 8dB and 0Hz, respectively. BPSK and QPSK modulations are recognized with 99% accuracy with 25 received symbols while 75 received symbols are required to achieve the same accuracy with 8PSK. This trend—where 8PSK is recognized less accurately than BPSK and QPSK, given the same number of received symbols—persists even at higher SNR levels.

Active-mode (mis)detection performance Figure 8 shows the detection probability of the all the possible

modulation schemes that can be used in active-mode Aileron. BPSK and QPSK can be easily distinguished from each other but when the received symbols are modulated using 8PSK, approximately 22% of the symbols are mis-recognized as QPSK. This error is due to the increased variance in the MSE differences used by the detection rules that is brought about by the multipath fading channel.

Passive-mode Aileron accuracy. Figure 9 shows the accuracy of passive-mode Aileron when applied to data subcarriers from a single OFDMA subchannel. Since there are are 32 data subcarriers in each OFDMA subchannel, 10 OFDM blocks will give 320 data symbols—significantly more than that obtained from the by active-mode Aileron. The larger number of received data symbols increases the accuracy of Aileron: BPSK modulation is recognized with accuracy 100% of the time at SNRs greater than 2dB while perfect identification of QPSK and 8PSK occur at SNRs above 10dB and 16dB, respectively. The AMR algorithm can always differentiate between the PSK modulations: mis-identified QPSK and 8PSK modulations are always labeled as QAM, rather than another PSK scheme.

For the QAM schemes, 64QAM is accurately identified at all SNR levels while 16QAM is correctly identified only up until 12dB, above which the recognition accuracy of 16QAM encounters a significant drop as it is consistently mis-identified as QPSK. This is because at higher SNRs, the mean value of $\mathrm{MSE}_{\mathrm{QPSK}}(S) - \mathrm{MSE}_{\mathrm{8PSK}}(S)$, $\mathrm{MSE}_{\mathrm{QPSK}}(S) - \mathrm{MSE}_{\mathrm{16QAM}}(S)$ and $\mathrm{MSE}_{\mathrm{16QAM}}(S) - \mathrm{MSE}_{\mathrm{64QAM}}(S)$ of a 16QAM-modulated input converges, as seen in Figure 5d. With an AMR window size of 10 OFDM blocks, the variance of MSE differences is large enough for 16QAM to be mistaken for QPSK with a high probability. If we double the input AMR window size to 20 blocks, 16QAM will be identified with perfect accuracy, as shown in Figure 10.

4.3 Aileron Accuracy in Mobile Environments

Mobility in wireless networks is characterized by the presence of doppler shift in transmissions over the channel. The comparative performance of Aileron with respect to the different input modulations in a mobile environment is similar to that described in Section 4.2, albeit with different accuracy values.

Figure 11 shows the lowest SNR at which active-mode Aileron can achieve 90% accuracy for BPSK, QPSK and 8PSK modulations under different mobility speeds. The accuracy of Aileron is computed using 50000 AMR windows, each with a length of 50. In this environment, BPSK and QPSK modulations can be correctly identified

90% of the time at SNR greater than 10dB and 7dB, respectively, while greater than 90% accuracy in recognizing 8PSK is achieved for all the considered SNR levels and doppler shifts.

Figure 12 shows the results of minimum SNR at which passive mode Aileron can achieve 90% accuracy. We use an AMR window size of 10. At SNR greater than 12dB, BPSK and QPSK can be correctly recognized with 90%, while at 22dB SNR and above, 8PSK can be recognized with 90% accuracy with a doppler frequency of up to 800Hz.

4.4 Discussion

The above results show that for an indoor environment with little to no mobility, only 10 OFDM blocks are necessary for BPSK and QPSK modulations to be identified with 99% accuracy at an SNR of 14dB and higher. Hence, if reliable and fast signaling is necessary over a large SNR range, information can be transmitted using a binary number system with BPSK and QPSK, representing 0 and 1 respectively, as the modulation basis. However, if some signaling error can be tolerated (up to 20%) or the SNR is expected to be high, then a more compact, ternary number system can be used instead. Given a fixed number of subcarriers, the addition of 8PSK as a supported modulation scheme increases the transmitted signaling rate, but also increases the receive error. A detailed analysis of the rate-error tradeoff is beyond the scope of this paper.

The reliability of active-mode Aileron extends even to the case of mobile networks—Aileron can achieve a high recognition accuracy even in the case of high mobility, thus making modulation-based signaling feasible for mobile networks. We stress that only 50 OFDM symbols are necessary to decode a ternary number over with a doppler shift of 800Hz (which is roughly equivalent to a speed of 80m/s).

Our results also show that the passive-mode Aileron can recognize subcarrier modulations accurately over a large range of SNR values and mobility speeds. Hence, with only a small overhearing overhead of 10 OFDM symbols, a listening node can quickly and easily determine the transmission rates of all neighboring nodes, even if it cannot demodulate and recover the exact transmitted bits due to channel distortion. It must be stressed that this level of accuracy is achieved *without the need for a header or preamble*. Modulation detection does not require any frame level synchronization or channel correction support beyond what is already available in every basic OFDM block.

5   Real-World Evaluation

We have implemented Aileron on the USRP2 platform using the GNURadio library. In real-world experiments, Aileron can correctly detect BPSK, QPSK and 8PSK with an accuracy of 100%, 98% and 86% respectively. We will leave the full evaluation of this implementation to future work.

6   Related Work

Control Channel Design. Typical control channels can be classified to be in-band or out-of-band. In-band control channels carry control frames in the same channel as that used for data frames. This simple approach has led to applications that vary from in-band medium access control using CSMA [10] and slotted ALOHA [11] to in-band probe frames for auto-rate selection [5] and link-quality measurements in mesh networks [12]. Other approaches that transmit control frames using side-channels [13] and inter-frame gaps [14] also fall into this category. Out-of-band approaches are characterized by the use of a dedicated channel for control frames. If only one wireless interface is available [15], the need for it to be switched between the control and data channels incurs a significant coordination overhead. If multiple interfaces are available [16], the coordination overhead is reduced at the cost of higher hardware and power demands.

    Modulation Recognition. The method of modulation recognition in [8] is based on the differences of MSE, but its recognition algorithm is too simplistic to be able to differentiate PSK from QAM modulations. Other recognition methods include the use of higher-order statistics [17], wavelet transform [18], and cyclic features of the digital transmission [19].

7   Conclusion

In this paper, we have presented Aileron, a novel design for control channel in OFDM(A) wireless networks. Aileron is a new paradigm of communications which uses the *modulation type*, rather than the *symbol value*, to encode information. It is built upon the concept of modulation recognition and supports two modes of operation: (a) *active* mode, where ternary-valued control frames are sent over pilot subcarriers, and (b) *passive* mode, where the modulation rate of data subcarriers is automatically detected. This design has three unique features/advantages: (1) synchronization-free signaling, (2) low-overhead control frames transmission, and (3) resilience to errors. We have evaluated Aileron using both simulated and real-world channels to demonstrate both

its feasibility and reliability. We have demonstrated the applicability of Aileron to realistic networks by integrating it into FICA and showing how throughput and channel utilization can be increased with no additional temporal and spectrum overhead.

References

[1] L. Yang, W. Hou, L. Cao, B. Zhao, and H. Zheng, "Supporting Demanding Wireless Applications with Frequency-agile Radios," *NSDI*, 2010.

[2] K. Tan, J. Fang, Y. Zhang, S. Chen, L. Shi, and J. Zhang, "Fine-grained channel access in wireless LAN," in *SIGCOMM*, 2010.

[3] P. Bahl, R. Chandra, T. Moscibroda, R. Murty, and M. Welsh, "White space networking with wi-fi like connectivity," *ACM SIGCOMM Computer Communication Review*, vol. 39, pp. 27–38, Aug. 2009.

[4] Y. Yuan, P. Bahl, R. Chandra, and P. Chou, "Knows: Kognitiv networking over white spaces," *DySPAN*, 2007.

[5] H. Rahul, F. Edalat, D. Katabi, and C. Sodini, "Frequency-aware rate adaptation and MAC protocols," in *MOBICOM*, 2009.

[6] O. Dobre, A. Abdi, Y. Bar-Ness, and W. Su, "Survey of automatic modulation classification techniques: classical approaches and new trends," *Communications, IET*, vol. 1, no. 2, pp. 137–156, 2007.

[7] J. van de Beek, M. Sandell, and P. Borjesson, "ML estimation of time and frequency offset in OFDM systems," *IEEE Transactions on Signal Processing*, vol. 45, pp. 1800–1805, July 1997.

[8] M. Naik, A. Mahanta, R. Bhattacharjee, and HB, "An Automatic Blind Modulation Recognition Algorithm for M-PSK Signals Based on MSE Criterion," *E-business and Telecommunication Networks, Communications in Computer and Information Science*, vol. 3, pp. 257–266, 2007.

[9] "Technical report on rf channel characterization and system deployment modeling," Tech. Rep. JTC(AIR)/94.09.23-065R6, JTC (Air) Standards Contribution, Sept 1994.

[10] A. Woo and D. E. Culler, "A transmission control scheme for media access in sensor networks," *MOBICOM*, 2001.

[11] L. G. Roberts, "ALOHA packet system with and without slots and capture," *ACM SIGCOMM Computer Comm Review*, vol. 5, Apr. 1975.

[12] K. Kim and K. Shin, "On accurate and asymmetry-aware measurement of link quality in wireless mesh networks," *IEEE/ACM Transactions on Networking*, vol. 17, Aug. 2009.

[13] K. Wu, H. Tan, Y. Liu, J. Zhang, Q. Zhang, and L. Ni, "Side channel: bits over interference," in *MOBICOM*, 2010.

[14] K. Chebrolu and A. Dhekne, "Esense: communication through energy sensing," in *MOBICOM*, 2009.

[15] J. So and N. Vaidya, "Multi-channel mac for ad hoc networks: handling multi-channel hidden terminals using a single transc eiver," in *MobiHoc*, 2004.

[16] J. Wang, Y. Fang, and D. Wu, "A Power-Saving Multi-Radio Multi-Channel MAC Protocol for Wireless Local Area Networks," *INFOCOM*, 2006.

[17] A. Swami and B. Sadler, "Hierarchical digital modulation classification using cumulants," *IEEE Transactions on Communications*, vol. 48, Mar. 2000.

[18] K. Ho, W. Prokopiw, and Y. Chan, "Modulation identification of digital signals by the wavelet transform," *Radar, Sonar and Navigation, IEE Proceedings*, vol. 147, no. 4, 2000.

[19] B. Ramkumar, "Automatic modulation classification for cognitive radios using cyclic feature detection," *IEEE Circuits and Systems Magazine*, 2009.